J Comput Neurosci (2014) 36:67–79
DOI 10.1007/s10827-013-0469-1

Gap junction permeability modulated by dopamine exerts effects on spatial and temporal correlation of retinal ganglion cells' firing activities

Jing-Yi Bu · Hao Li · Hai-Qing Gong · Pei-Ji Liang · Pu-Ming Zhang

Received: 5 December 2012 / Revised: 20 May 2013 / Accepted: 29 May 2013 / Published online: 10 June 2013

Abstract Synchronized activities among retinal ganglion cells (RGCs) via gap junctions can be increased by exogenous dopamine (DA). During DA application, single neurons' firing activities become more synchronized with its adjacent neighbors. One intriguing question is how the enhanced spatial synchronization alters the temporal firing structure of single neurons. In the present study, firing activities of bullfrog's dimming detectors in response to binary pseudo-random checker-board flickering were recorded via a multi-channel recording system. DA was applied in the retina to modulate synchronized activities between RGCs, and the effect of DA on firing activities of single neurons was examined. It was found that, during application of DA, synchronized activities between single neuron and its neighboring neurons was enhanced. At the meantime, the temporal structures of single neuron spike train changed significantly, and the temporal correlation in single neuron's response decreased. The pharmacological study results indicated that the activation of D1 receptor might have effects on gap junction permeability between RGCs. Our results suggested that the dopaminergic pathway participated in the modulation of spatial and temporal correlation of RGCs' firing activities, and may exert critical effects on visual information processing in the retina.

Keywords Temporal correlation · Spatial correlation · Multi-channel recording · Retinal ganglion cell · Dopamine

Abbreviation

CCF	Cross-correlation function
DA	Dopamine
ISI	Inter-spike-interval
MEA	Micro-electrode array
RGC	Retinal ganglion cell
SCH	SCH-23390
SU	Sulpiride
TCI	Temporal correlation index

Action Editor: Barry Richmond

J.-Y. Bu · H. Li · H.-Q. Gong · P.-J. Liang · P.-M. Zhang (✉)
School of Biomedical Engineering, Shanghai Jiao Tong University, 800 Dong-Chuan Road, Shanghai 200240, China
e-mail: pmzhang@sjtu.edu.cn

1 Introduction

Population activities have been reported to contribute to visual information encoding of retinal ganglion cells (RGCs) (Brivanlou et al. 1998; Meister et al. 1995; Schnitzer and Meister 2003). Spatially correlated firing activity is one important aspect of population activities of RGCs. The spatial correlation, which can be categorized into several subtypes based on neuronal wiring, was extensively studied (Brivanlou et al. 1998; DeVries 1999). It was found that correlated firing activities between RGCs were induced by common inputs from bipolar or amacrine cells, while synchronized activities between the adjacent RGCs were mediated by gap junctions (Brivanlou et al. 1998). The spatial correlation among dimming detectors (one of the four subtypes of bullfrog RGCs based on their photo-response characteristics) showed dynamic variations during contrast adaptation, and the synchronized activities between dimming detectors via gap junctions exhibited dopaminergic modulation (Li et al. 2012). It was reported that dopamine (DA) could enhance the synchronization of dimming detectors' firing activities and the size of single neuron's receptive field was enlarged, which would result in the reduction of information details during coding visual scenes in the retina (Li et al. 2012). DA changes the gap junctional permeability (Bloomfield and Volgyi 2009) and the spiking of single neuron becomes more synchronized with its adjacent neighbors. The relative more frequent occurrence of synchronized activity reflects the potential changes in firing

sequence of paired single neurons. However, whether and how the DA-induced changes in synchronized activities exert effect on temporal structure of single neurons' spike trains is still unknown.

Temporal correlation reflects the features of temporal structure of single neurons' responses. Temporal correlation was thought to play an important role in information transmission in neural systems (Buonomano and Maass 2009) and it could improve coding performance in the presence of noise (Koch et al. 2004). Burst, which is characterized by consecutive spikes with relative short inter-spike-intervals (ISIs), is a distinctive component in neuronal spike sequence and substantially contributes to the temporal structure of single neuron firing activities. It was reported that bursts were an important part of the neural temporal coding. Bursts were supposed to contribute to the detection of stimulus features (Metzner et al. 1998; Reinagel et al. 1999; Lesica and Stanley 2004), and had enhanced ability to elicit post-synaptic neuron's firing (Lisman 1997; Swadlow and Gusev 2001; Krahe and Gabbiani 2004).

In the present study, we recorded activities of dimming detectors in bullfrog retinas by using multi-channel recording technique *in vitro*. With the application of DA, the gap junction conductance between dimming detectors was modulated. The effects of DA on neuron population responses were measured by calculating the spatial correlation strength between single neuron and its neighboring neurons, while influences of DA on single neuron spike trains were measured by examining the change of ISIs distribution. During the application of DA, the spatial correlation among RGCs increased significantly while the temporal structure of single neuron spike trains changed remarkably and the temporal correlation index (TCI) showed a reduction of temporal correlation of single neuron's response. The results showed that the gap junctions between neighboring RGCs played a key role in the spatial and temporal correlated firing activities and its permeability was regulated through the activation of dopaminergic pathway. Further investigation with application of DA receptor antagonists suggested that the dynamic changes in firing patterns might be caused by the activation of D1 receptors. Our results suggested that dopaminergic pathway participated in the modulation of spatial and temporal correlation of RGCs' firing activities, and may exert critical effects on visual information processing in the retina.

2 Materials and methods

2.1 Surgery

Bullfrogs were dark adapted for more than 30 min before experiments. Under a dim red light, the bullfrog was double pithed and its eyes were enucleated. The separated eyeball was then hemisected. The eyecup was cut into several small pieces and the retina was isolated carefully (Li et al. 2012; Jing et al. 2010). All animal experiments were performed in accordance with regulation of Ethics Committee, School of Biomedical Engineering, Shanghai Jiao Tong University (No. 2012029).

The isolated retina was attached on a piece of micro-electrode array (MEA, MCS GmbH, Germany) with ganglion cell layer contacting the electrodes. The normal oxygenated (95 % O_2 and 5 % CO_2) Ringer's solution (containing in mM: 100.0 NaCl, 2.5 KCl, 1.6 $MgCl_2$, 2.0 $CaCl_2$, 25.0 $NaHCO_3$, 10.0 glucose) superfused the retina on MEA. In pharmacological experiments, DA (1 μM), sulpiride (SU, 10 μM) and SCH-23390 (SCH, 10 μM) were applied with the Ringer's Solution. All drugs were purchased from Sigma-Aldrich (St. Louis, MO, USA).

2.2 Multi-channel recording

The MEA was composed of 60 electrodes (10 μm in diameter, horizontal and vertical tip-to-tip distance between neighboring electrodes was 100 μm) which were arranged in an 8×8 matrix with 4 corners void. The ambient temperature was maintained at 22 °C–24 °C. A tiny Ag/AgCl pellet with wire was immersed into the perfusate as a reference electrode.

The neuronal signals were recorded by the MEA and amplified through a 60-channel amplifier (single-ended, 1,200×, input impedance $>10^{10}$ Ω, output impedance 330 Ω). After amplification, neuronal signals were sampled at a rate of 20 kHz for each channel. The acquired data were stored in a computer for offline analysis. Spikes were sorted by principal component analysis (Wang et al. 2006; Zhang et al. 2004). K-means clustering method was used to identify the data corresponding to spikes as well as OfflineSorter (Plexon Inc. Texas, USA). Only single-neuron events clarified by all the spike sorting methods mentioned above were used for subsequent analyses (Chen et al. 2004; X. Liu et al. 2007; Li et al. 2012).

There are four subtypes of bullfrog retinal ganglion cells classified by their photo-response properties: dimming detector, moving-edge detector, contrast detector, and convexity detector (Lettvin et al. 1959). In our experiments, we only analyzed dimming detectors whose response to light-off stimulation was sustained firing and receptive field had an off-center (Li et al. 2012).

2.3 Stimulation

Visual stimuli were applied via a computer monitor (796 FD II, MAG, 1,024×768 pixels), focused on an area of 0.9×0.9 mm^2, and projected to the isolated retina attached on MEA through an optical system.

The pseudo-random checkerboard flickering sequence was applied to study the correlation characteristics of RGC's activities. Each frame was constituted of 16×16 sub-squares (56 μm×56 μm), every one of which was set a value either "1" (12.18 nw/cm^2 in luminance) or "−1" (0.00 nw/cm^2 in luminance) taken from an m-sequence (Reid et al. 1997). The frame rate was 20 Hz and the duration of a whole stimulus was 250 s.

2.4 Spatial correlation strength

In our experiments, DA influenced the gap junction conductance between adjacent dimming detectors which was the physiological basis of synchronized spiking of two neighboring neurons. Cross-correlation function (CCF) was calculated to measure the synchronization strength between two time series. With a resolution of 1 ms (no more than 1 spike existed in 1 bin), a spike train was binned into a "0–1" sequence in which "1" stands for a spike and "0" for none. Given "0–1" spike sequences x and y, the normalized CCF was calculated as follows:

$$C_{xy}(m) = \frac{\sum_{n=0}^{N-|m|-1} x_n y_{n+m}}{R} \quad where\ R = \sqrt{\sum_{i=1}^{N} x_i^2 \sum_{i=1}^{N} y_i^2} \quad (1)$$

where x_n denotes the value of sequence x at the moment n; y_{n+m} denotes the value of sequence y at the moment $n+m$; N is the length of "0–1" sequence; R is the normalization factor; $C_{xy}(m)$ is the normalized CCF coefficient of sequences x and y with a lag of m. When the normalized CCF coefficient reaches its maximum, the lag m is defined as the time delay of the two binned spike trains x and y. It reflects a maximal synchronization of two sequences when the preceding one was postponed for lag m.

The mean of cross correlation function between two spike trains is defined as

$$mean = \frac{1}{2M+1} \sum_{m=-M}^{M} C_{xy}(m) \quad (2)$$

where $C_{xy}(m)$ is cross correlation function of sequence x and y, M is the maximum of time lag m when computing $C_{xy}(m)$. SD is the standard deviation of the cross correlation function $C_{xy}(m)$ and it is defined as

$$SD = \sqrt{\frac{1}{2M} \sum_{m=-M}^{M} \left(C_{xy}(m) - mean\right)^2} \quad (3)$$

We focused on the precisely synchronized firing activities of recorded RGCs which were characterized by a sharp peak at zero-lag in the CCF (with peak value > mean + 10SD, examples were shown in Fig. 1a and c). With a resolution of 0.05 ms, the fine structure of CCF can be detected. There were two subtypes of synchronized activities recorded in our experiments: dual-peak induced by mutual excitation between two RGCs through the gap junction (Fig. 1b) and one-peak induced by the asymmetry of the gap junction conductance or the different membrane state of two RGCs (Fig. 1d). Both of these two kinds of synchronization were mediated by gap junctions (Brivanlou et al. 1998; Li et al. 2012) and all of the neurons analyzed in this paper had this kind of synchronized activity with at least one neighboring neuron.

At the same time, the number of synchronized firing neurons of each single dimming detector was also counted to measure the spatial correlation strength. Large synchronized neuron number implied strong spatial correlation between the neuron and its surrounding neurons, and *vice versa*.

2.5 Temporal correlation index

TCI was calculated to estimate the temporal correlation of neurons' firing activities which had been used in our previous work (W. Z. Liu et al. 2011a). It was estimated based on an entropy estimation method proposed by Strong and his co-workers (Strong et al. 1998; Reinagel and Reid 2000). Spike sequences of "0–1" were generated using 2-ms-bin (to ensure that each bin has no more than 1 spike) where "1" meant there was a spike at that time bin while "0" without a spike. Firstly, with an assumption that each firing activity was temporally uncorrelated from the others, the entropy rate (in units of bits per sec) of a spike train denoted H_M was calculated with 1-bin length "word" as follows:

$$H_M = -\frac{1}{\Delta\tau}(P_1 \log_2 P_1 + P_0 \log_2 P_0) \quad (4)$$

where P_1 and P_0 denote the probabilities of "1" and "0" occur in a binned spike train respectively, and $\Delta\tau$ is bin width which is fixed to 2 ms.

Then the real entropy rate of the binned spike train denoted H_r which considered the internal temporal correlation in the sequence was calculated following the method proposed by Strong *et al*. (Strong et al. 1998). Briefly, entropy rate with word length ≥2 bins were calculated and plotted against the reciprocals of word length, the linear part of which can be fitted as:

$$H(n) = H_r + \frac{H_1}{n} + \frac{H_2}{n^2} \quad (5)$$

where n is the word length, $H(n)$ is the calculated entropy rate, and H_r is the estimated real entropy rate. $\frac{H_1}{n}$ and $\frac{H_2}{n^2}$ are corrections for the bias of estimated entropy caused by finite data set.

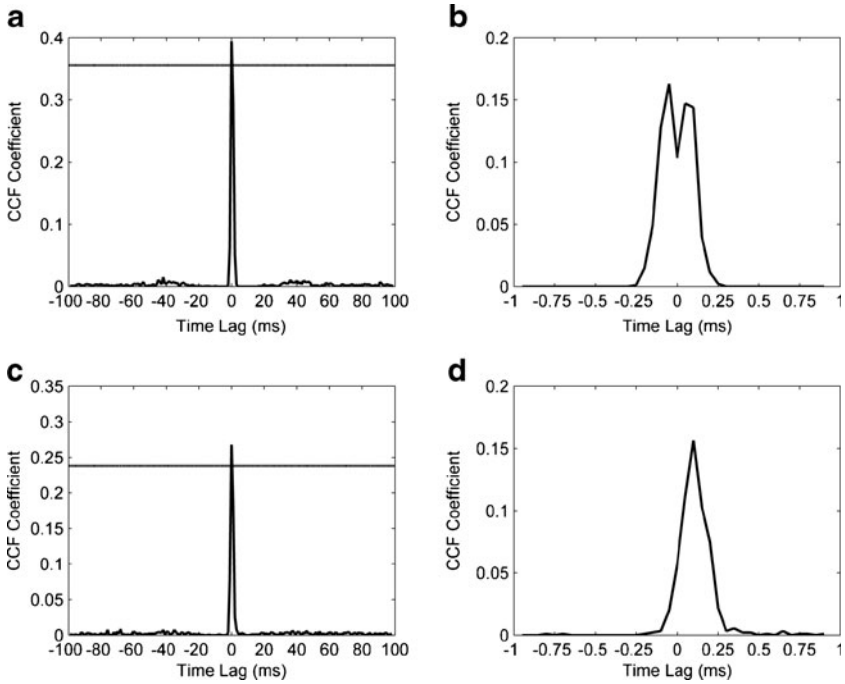

Fig. 1 Two examples of CCF of precisely synchronized neuron pairs. (**a**) CCF of one synchronized neuron pair (bin= 1 ms). The dashed line showed 'mean + 10SD' boundary. (**b**) The fine structure of CCF (the same neuron pair in **a**, bin= 0.05 ms). It had dual peaks at the time lags of 0.05 ms and −0.05 ms. (**c**) CCF of another synchronized neuron pair (bin=1 ms). The dashed line showed 'mean + 10SD' boundary. (**d**) The fine structure of CCF (the same neuron pair in **c**, bin=0.05 ms). It had one peak at the time lag of 0.1 ms

TCI was the discrepancy between H_M and H_r:

$$TCI = H_M - H_r \tag{6}$$

Insufficient data may result in biased estimation for entropy. In order to ascertain data adequacy, we followed the method proposed by Strong *et al*. (Strong et al. 1998). The data were rejected as inadequate if the difference between extrapolated infinite-data size entropy and the calculated whole-sequence size entropy was more than 20 % of the infinite-data size entropy (Strong et al. 1998). All data presented in this paper were adequate according to this criterion.

3 Results

3.1 Effects of DA on RGCs' synchronous activities

DA, as a neural modulator whose release is light-dependent in retina (Witkovsky 2004; Witkovsky et al. 1993), has been implicated in playing key roles in the regulation of gap junction conductance (Bloomfield and Volgyi 2009; Ribelayga et al. 2008; Mills et al. 2007; Hampson et al. 1992). In our experiments, exogenous DA (1 μM) was applied to modulate dimming detectors' synchronized activities.

Figure 2 shows an example of the firing rate changes of a dimming detector in response to sustained checkerboard flickering (time window=1 s) in the normal Ringer's solution (Fig. 2a) and with DA application (Fig. 2b) respectively. Decreases in firing rate over time were observed in both conditions, suggesting that the DA application did not change the property of adaptation process of single neuron's firing activity much (Li et al. 2012).

It has been well demonstrated that gap junction coupling is responsible for the synchronized activities between neighboring RGCs (Brivanlou et al. 1998). In our present study, two indices were chosen to describe the strength of synchronization strength between adjacent RGCs: peak value of CCF of each paired dimming detectors and the synchronized neuron number for each single dimming detector.

CCF values of each paired dimming detectors were calculated. Paired dimming detectors that showed synchronous activities in both control and DA conditions were chosen for analysis (113 neurons, 254 neuron pairs from 4 retinas). For each paired dimming detectors, a single square is plotted based on the peak value of CCF during control (abscissa) *versus* that during DA (ordinate) (Fig. 3a–b). The majority of squares fell above the diagonal, indicating that with the application of DA, the peak values of CCF of dimming detectors increased significantly (0.33±0.01 (control), 0.41± 0.01 (DA), mean ± S.E., $p<0.01$, paired *t*-test, $n=254$) .

The number of synchronized neurons for each single neuron was counted. Figure 3c–d showed the results of the same 113 neurons from the 4 retinas. A single triangle represents a neuron, whose abscissa and ordinate are the number of its synchronized neurons before and during the use of DA respectively. This index increased significantly (3.44±0.22 (control), 4.09±0.26 (DA), mean ± S.E., $p<0.01$, paired *t*-test, $n=113$), which suggested that the strength of synchronization in neuron population activity enhanced in DA conditions.

In conclusion, with the application of DA, synchronized activities between single neuron and its surrounding neurons

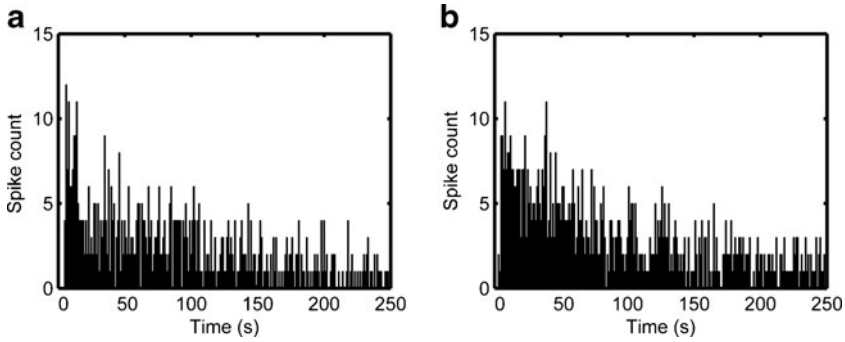

Fig. 2 Time-dependent firing rate changes. (**a**) & (**b**) Time-dependent firing rate of an example dimming detector during control and DA application, respectively (time window=1 s)

mediated by gap junction were enhanced. The results showed that the spatial correlation of RGCs was enhanced by exogenous DA. Since it was reported that the size of single neuron's receptive field was positively related to the strength of its synchronized activity with its neighboring neurons (Li et al. 2012), our results suggested that the details of visual information would be reduced somewhat during encoding process in the retina with the application of DA.

3.2 Effects of DA on spike train structure of single neurons

Since the spatial correlation strength mediated by gap junction were enhanced during DA application, the spiking of single neuron became more synchronized with its neighboring neurons and the structure of single neuron spike train would inevitably change.

ISI histogram was used to examine the distribution of intervals between spikes in a spike train. Data from the same 4 retinas were analyzed and the result of one retina (21 neurons) is shown in Fig. 4a. The proportion of small ISIs (<6 ms) was reduced during the use of DA (Fig. 4a). According to the identification criterion of burst (distinguished from single spikes) that ISI <6 ms (W. Z. Liu et al. 2011a; W. Z. Liu et al. 2011b), the result suggested the number of burst in the firing activities of RGCs was reduced.

Furthermore, the distribution of successive pairs of ISI of one neuron spike train was analyzed. For each spike, a single point is plotted based on the preceding ISI (abscissa) *versus* the subsequent ISI (ordinate) and the results were shown in Fig. 4b–c.

During control, a distinct firing pattern was observed that there were a large number of burst activities in the spike train. The area within a box at the bottom of Fig. 4b was a cluster of the first spike of bursts: a preceding interval >10 ms, and a subsequent interval <6 ms. Those lying at the bottom left corner were spikes within bursts (with previous and subsequent intervals

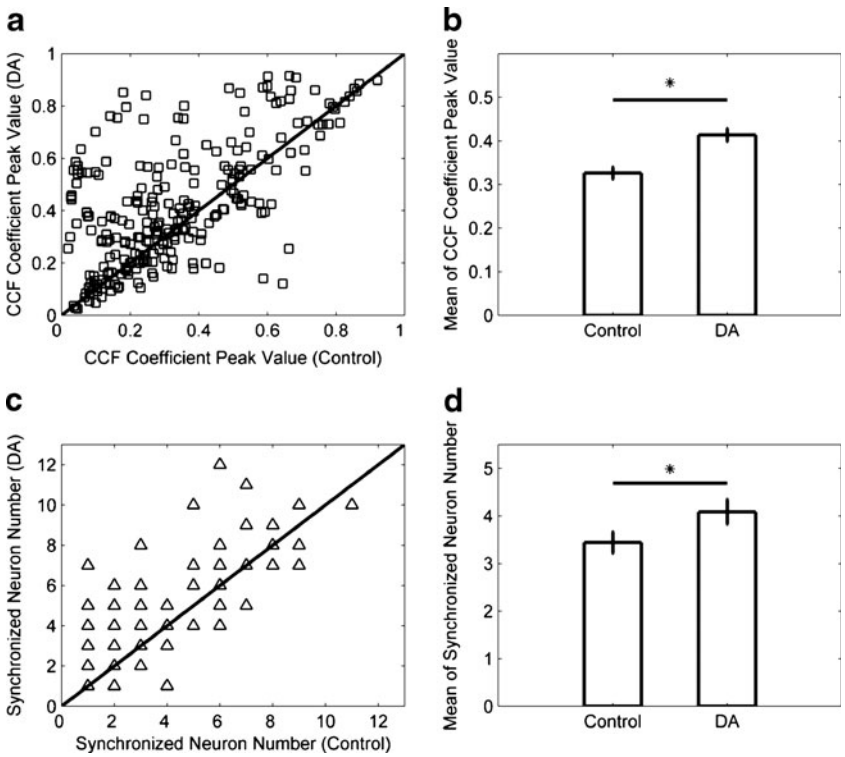

Fig. 3 Synchronization activity under control and DA conditions. (**a**) Comparison of CCF peak value during control and DA application (113 neurons, 254 neuron pairs from 4 retinas). (**b**) Bar plots showing mean CCF peak value during control and DA application respectively (mean ± S.E., paired *t*-test, *, $p<0.01$, $n=254$). (**c**) Comparison of the synchronized neuron number of each single neuron during control and DA (the same 113 neurons from the 4 retinas). (**d**) Bar plots showing mean synchronized neuron number for control and DA respectively (mean ± S.E., paired *t*-test, *, $p<0.01$, $n=113$)

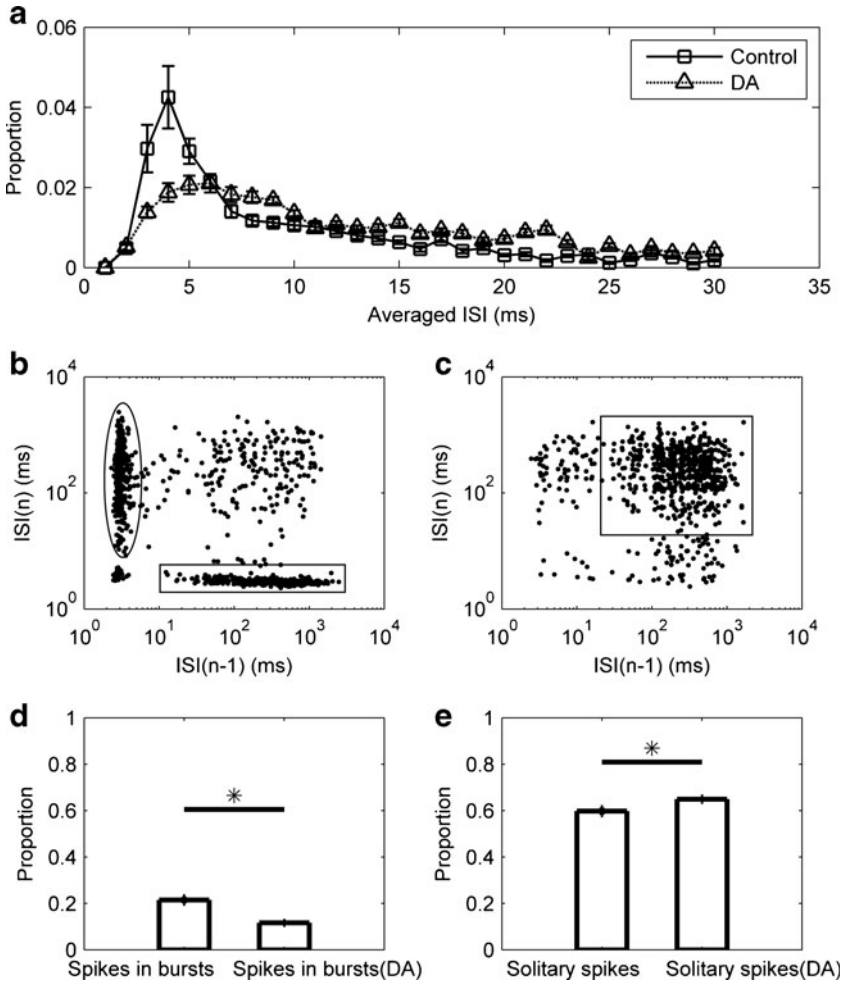

Fig. 4 ISI distribution. (**a**) Comparison of averaged ISI distribution of one retina (21 neurons) during control (square, solid-line, mean ± S.E.) and DA application (triangle, dash-line, mean ± S.E.). (**b**) & (**c**) Previous *vs*. subsequent ISI of one neuron during control and DA application respectively. (**d**) Bar plots showing proportion of spikes in bursts during control and DA application respectively (mean ± S.E., paired *t*-test, *, $p<0.01$, $n=113$). (**e**) Bar plots showing proportion of solitary spikes during control and DA application respectively (mean ± S.E., paired *t*-test, *, $p<0.01$, $n=113$)

both <6 ms). The area circled by an ellipse represented the final spikes of bursts which were followed by a long interval >10 ms. However, there are no clusters near the coordinate axes in DA condition as shown in Fig. 4c. In the center of the plot, there was a big cluster (within the box) of single spikes with preceding and subsequent intervals both >20 ms. Across the 113 neurons, proportion of spikes in bursts decreased significantly (Fig. 4d, 0.21±0.01 (control), 0.12±0.01 (DA), mean ± S.E., $p<0.01$, paired *t*-test, $n=113$), while the proportion of solitary spikes increased significantly (Fig. 4e, 0.60±0.02 (control), 0.65± 0.01 (DA), mean ± S.E., $p<0.01$, paired *t*-test, $n=113$), with the application of DA. The result suggested that with the use of DA, spikes within single neuron's response became more independent and the number of burst activities reduced remarkably.

The ISI distributions of neurons' firing activities of the other 3 retinas were almost similar as shown in Fig. 4. The results showed that during the application of DA, the number of bursts in single neuron spike trains was reduced. As we known, bursts played an important role in temporal correlation of spike trains and they were supposed to contribute to the stimulus feature encoding and information transmission (Krahe and Gabbiani 2004). So, the reduction of bursts in spike trains potentially affected the temporal coding efficiency of RGCs.

3.3 Effects of DA on temporal correlation

Temporal correlation is a key indicator to reflect the temporal structure of spike trains and it has been reported that this kind of correlation contributed to visual information coding of RGCs.

TCI, one of the indices of temporal correlation, was then calculated to measure the temporal correlation of each single neuron's response before and during the application of DA. It was calculated as the difference between the "maximum" entropy rate (obtained by assuming each spike is independent) and the real entropy rate (estimated by Eq. 5) of a spike train. TCI measured the predictability of one time bin of the response from the rest of the response (Reinagel and Reid 2000). TCI with large value reflected strong dependence of one time bin on the others. So TCI can reflect temporal correlation to some extent, and large value implied strong temporal correlation within a spike train, and *vice versa*.

Figure 5 showed the results for the same 113 neurons recorded from the 4 retinas. It was found that the temporal

correlation in a single spike train was remarkably decreased during the use of DA. Decreased TCI values were found in 85 cells (75.22 %, Fig. 5a). The mean values of TCI values (across the 113 cells) were 1.00±0.11 (during control) and 0.41±0.05 (during DA) (mean ± S.E.) respectively, which were significantly different ($p<0.01$, paired t-test, $n=113$, Fig. 5b). Reduced TCI values reflected that the temporal correlation within spike trains decreased and suggested that the visual information encoded and transferred by temporal correlation in spike trains would be lost to a certain extent during the application of DA.

3.4 D1 receptor affects the modulation of spatial and temporal correlation

D1 and D2 DA receptors were found to be involved in modulating the coupling among RGCs (Hu et al. 2010). To examine the effects of D1 and D2 receptors in DA-induced influence on spatial and temporal correlation, D1 and D2 receptor antagonists were applied in our experiments.

With the application of D2 receptor antagonist SU (10 μM), data of 39 neurons (55 neuron pairs) from 3 retinas were analyzed, and the results were shown in Fig. 6. A significant increase was observed in the CCF value of the majority of paired RGCs (0.36±0.03 (control), 0.43±0.03 (SU), mean ± S.E., $p<0.01$, paired t-test, $n=55$, Fig. 6b) and for each cell's synchronized neuron number, a significant increase was also observed (2.26±0.20 (control), 2.77±0.27 (SU), mean±S.E., $p<0.05$, paired t-test, $n=39$, Fig. 6d). Decreased TCI values were found in 35 neurons (90 %, 39 neurons in total, Fig. 6e). The mean values of TCI values (across the 39 neurons) were 1.32±0.22 (control) and 0.18±0.02 (SU) respectively, which were significantly different ($p<0.01$, paired t-test, $n=39$, Fig. 6f). So, the application of SU produced a significant increase in the synchronization, and it showed similar effects on the firing activity of dimming detectors as DA.

In this set of experiment, the application of SU inhibited D2 receptors whilst allowed D1 receptors being activated by endogenously released DA. Thus, it suggested that the enhancement on gap junction connection might be dependent on D1 receptor-dependent cascade.

To further clarify the role of DA receptors, D1 receptor antagonist SCH (10 μM) was applied. Data of 21 neurons from 3 retinas (16 neuron pairs) were analyzed and the results were shown in Fig. 7. Synchronization activity of dimming detectors didn't show a significant change, neither CCF peak value (0.34±0.06 (control), 0.39±0.04 (SCH), mean ± S.E., $p>0.05$, paired t-test, $n=16$, Fig. 7b) nor synchronized neuron number (1.71±0.16 (control), 2.14±0.27 (SCH), mean ± S.E., $p>0.05$, paired t-test, $n=21$, Fig. 7d). During control, the mean value of TCI was 0.21±0.03. With the application of SCH, the mean value of TCI was 0.18±0.03, and it showed insignificant decrease ($p>0.05$, paired t-test, $n=21$, Fig. 7f). When D1 receptors were blocked by SCH and only D2 receptors were activated by endogenous DA, the significant increase in the synchronization and the significant decrease in TCI during DA/SU were attenuated. The results indicated that the activation of D2 receptors by endogenous DA didn't have notable effects on gap junction connection between RGCs, and could not trigger a significant change in firing activities of RGCs.

These results, together with the DA/SU experiments results, testified that DA-induced influence on spatial and temporal correlation of firing activities of dimming detectors might be due to the activation of D1 receptors. It was inferred that, when the D1 receptors were activated, the spatial correlation among RGCs were enhanced and the temporal correlation among single RGC's firing activities were reduced. It suggested that the information encoding efficiency in the retina would be weakened by the activation of D1 receptors.

4 Discussion

Spatial pattern among neuronal populations and temporal pattern in single neuron spike trains before and during the application of DA were investigated in the present study. The results showed that with DA, the spatial correlation pattern among adjacent RGCs increased while temporal correlation pattern for the majority of single neurons reduced significantly, which

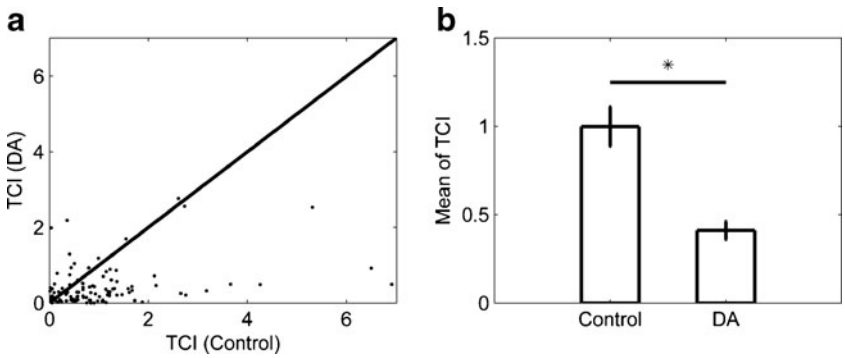

Fig. 5 TCI during control and DA application. (**a**) Comparison of TCI of 113 neurons from 4 retinas during control and DA application. (**b**) Bar plots show mean TCI during control and DA application and error bars represent S.E.. Significant difference is marked by asterisks (*, paired t-test, $p<0.01$, $n=113$)

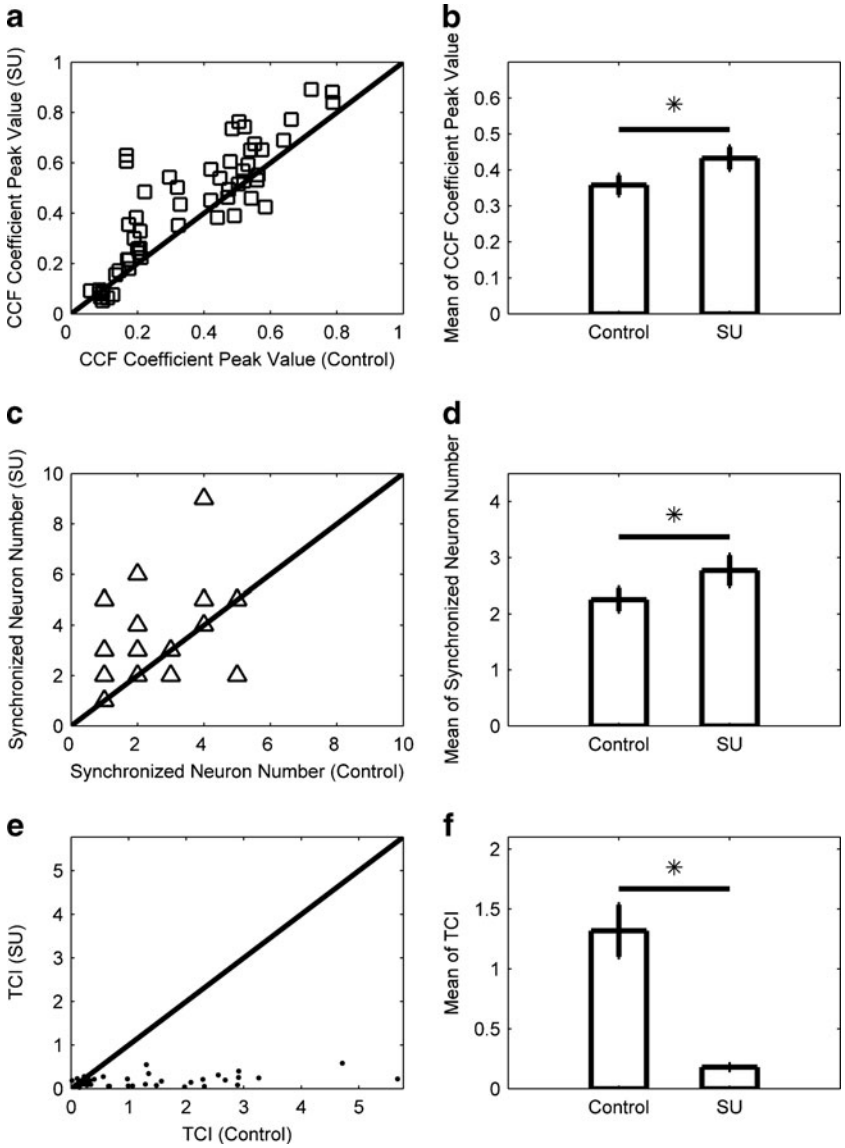

Fig. 6 Synchronization activity and TCI under SU condition. (**a**) Comparison of CCF peak value during control and SU application (39 neurons, 55 neuron pairs from 3 retinas). (**b**) Bar plots showing mean CCF peak value for control and SU application respectively (mean ± S.E., paired *t*-test, *, $p<0.01$, $n=55$). (**c**) Comparison of the synchronized neuron number of each single neuron during control and SU application (the same 39 neurons from 3 retinas). (**d**) Bar plots showing mean synchronized neuron number during control and SU application respectively (mean ± S.E., paired *t*-test, *, $p<0.05$, $n=39$). (**e**) Comparison of TCI during control and SU application (39 neurons from 3 retinas). (**f**) Bar plots showing mean TCI for control and SU application respectively (mean ± S.E., paired *t*-test, *, $p<0.01$, $n=39$)

assumed that DA exerts effects on these two kinds of correlation patterns. In addition, the results of DA analogist experiments suggested that D1 receptors might play a role in this phenomenon.

4.1 Spatial correlation and temporal correlation

Population activity of RGCs has been proposed to play an essential role in visual information encoding (Brivanlou et al. 1998; Meister et al. 1995; Schnitzer and Meister 2003). It was reported that correlated activities of RGCs may drive their post-synaptic neurons in lateral geniculate nucleus more efficiently (Field and Chichilnisky 2007; Usrey et al. 1999), suggesting that the spatial correlation makes the transmission of visual information more efficiently. In the present work, our results showed that during DA application the spatial correlation among RGCs enhanced. Consequently, the information transmission to the postsynaptic neurons might be more efficiently. However, our previous work had demonstrated that when the spatial correlation among RGCs enhanced, the single neuron's receptive field would be enlarged and the information details encoded in the retina would lose to some extent (Li et al. 2012).

In addition to spatial correlation among RGC population, temporal correlation in single neuron spike trains has been extensively documented in various parts of the nervous system, including visual system (Teich et al. 1996), which demonstrated that spike events were not totally isolated from each other. In guinea pig RGCs, temporal correlation was proposed to improve coding performance in the presence of noise (Koch et al. 2004). Furthermore, it was reported that the RGC may encode visual information in a predictive way (Hosoya et al. 2005), implying that information is encoded not only based on the present input but also the recent firing history of the neurons. Temporal correlation can be regarded as memory for predictive coding behavior in this sense. Our

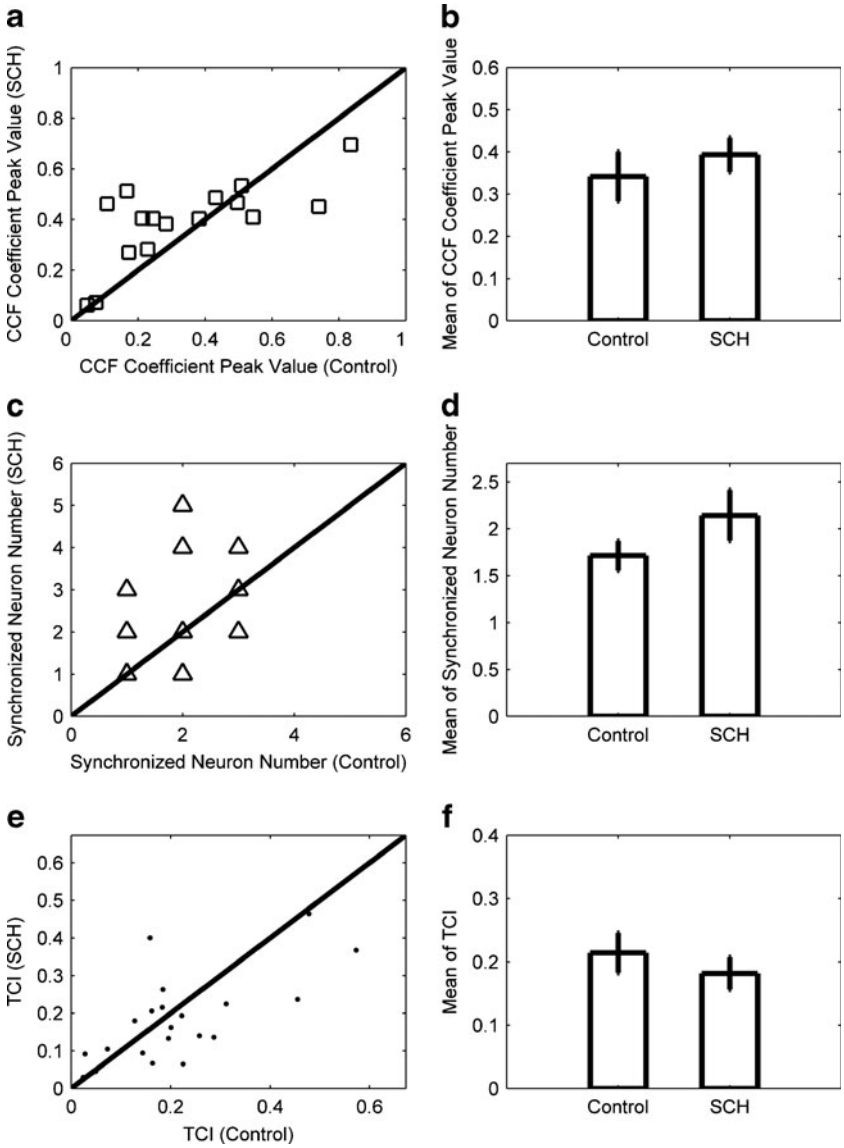

Fig. 7 Synchronization activity and TCI under SCH condition. (**a**) Comparison of CCF peak value during control and SCH (21 neurons, 16 neuron pairs from 3 retinas). (**b**) Bar plots showing mean CCF peak value for control and SCH respectively (mean ± S.E., paired *t*-test, $p>0.05$, $n=16$). (**c**) Comparison of the synchronized neuron number of a single neuron during control and SCH (21 neurons). (**d**) Bar plots showing mean synchronized neuron number during control and SCH respectively (mean ± S.E., paired *t*-test, $p>0.05$, $n=21$). (**e**) Comparison of TCI of 21 neurons from 3 retinas during control and SCH application. (**f**) Bar plots showing mean TCI during control and SCH (mean ± S.E., paired *t*-test, $p>0.05$, $n=21$)

results showed that during DA/SU application, the number of bursts and the temporal correlation in single neuron's firing activities decreased notably. So, it was inferred that the features encoded and transferred by the temporal correlation in neuron's firing activities would be weakened under unconventional DA conditions, including saturation concentration of DA or activation of D1 receptors.

Spatial correlation and temporal correlation are related to some extent. It was reported that the spatial and temporal correlations could improve retina's coding capacity (Pillow et al. 2008) and they were highly positively correlated in normal condition (W. Z. Liu et al. 2011a). In the present study, DA was applied to change the gap junction permeability, and then altered the state of the neural network of the retina. It was observed that these two kinds of correlations, namely the spatial correlation reflected by peak values of CCF and synchronized neuron number, and temporal correlation reflected by TCI values, changed towards the opposite directions during the application of DA. The spatial correlation increased while the temporal correlation decreased significantly. However, even the changing directions were different, these two kinds of correlations were positively correlated before and during the application of DA, in accordance with our previous results (W. Z. Liu et al. 2011a). The decrease of TCI values would impair coding performance in the present of noise (Koch et al. 2004), and some information features and transformation efficiency would be lost during encoding the visual scenes (Krahe and Gabbiani 2004). In the meantime, the increase of spatial correlation suggested that the transmission of encoded visual information became more effective, but some information details would be lost because of the enlarged size of RGC's receptive field (Li et al. 2012). In consideration of the DA's daily rhythm of its release (Witkovsky et al. 1993; Bloomfield and Volgyi 2009), the retina may chose different encoding strategy for input visual stimulus based on various environments.

4.2 Adaptation and temporal structure

RGCs recorded in our experiments showed the phenomenon of adaptation to contrast which referred to that the firing rate decreased progressively during response to steady contrast stimulus, and this phenomenon had been well observed (Baccus and Meister 2002; Chander and Chichilnisky 2001). In our experiments, the flickering checkerboard was regarded as sustained contrast stimulation. The mean intensity was maintained constant, while the stimulus contrast was set as 100 % (Li et al. 2012). We looked into the adaptation process to check whether the reduction of TCI values was caused by the adaptation or not.

The neurons' firing rate decreased and reached a steady state both in control and DA conditions (an example was shown in Fig. 2). The neurons' responses were partitioned into early- and late-adaptation processes simply by the midpoint of the spike sequence and the change of structures of these two parts were investigated. As the data acquired from half of a spike sequence are not adequate, we cannot calculate the TCI value directly for the early- and late-adaptation periods. So we analyzed the distribution of ISIs, and Fig. 8 shows the result of a single neuron as an example. The calculation of the other neurons showed similar results.

During control, the dots and crosses were clustered near coordinates both in early-(point, Fig. 8a) and late-(cross, Fig. 8b) adaptation period. It showed that the distributions of pairs of ISIs in these two periods were hardly different. With the application of DA, the dots and crosses near coordinates reduced and that in the central of the plot increased both in early-(points, Fig. 8c) and late-(crosses, Fig. 8d) adaptation period compared to that during control respectively. So, the structure of spike sequence changes little in early-and late-adaptation no matter in control or DA condition. In other words, the reduction of TCI values was not caused by the phenomenon of contrast adaptation.

4.3 TCI and synchronized neuron number

In the present study, it was found that temporal correlation reduced and spatial correlation increased during the application of DA. To investigate the underlying connection between these two kinds of correlations, the relationship between the TCI value and the synchronized neuron number of a single cell was studied. Figure 9 showed the result for 113 neurons recorded from 4 retinas, the same neurons for the previous analysis. It was clear that the TCI values had a tendency of decrease when the neuron had a large synchronized neuron number both in control (Fig. 9, square, solid-line) and DA condition (Fig. 9, triangle, dash-line). It can be inferred that it was the redistribution of electricity that caused the reduction of temporal correlation and the increase of spatial correlation after the application of DA. For a neuron, its electricity would flow into its gap junction coupled neurons when it released an action potential, and then it would have less chance to release a burst. The more gap junction coupled neurons one neuron had, the more neurons it synchronized, and the less bursts it released, thus resulted in a low TCI value. In our experiments, the exogenous DA increased the conductance of gap junction between dimming detectors, and the electricity became more dispersive. As a result, the synchronized neuron number increased (Fig. 3c–d)

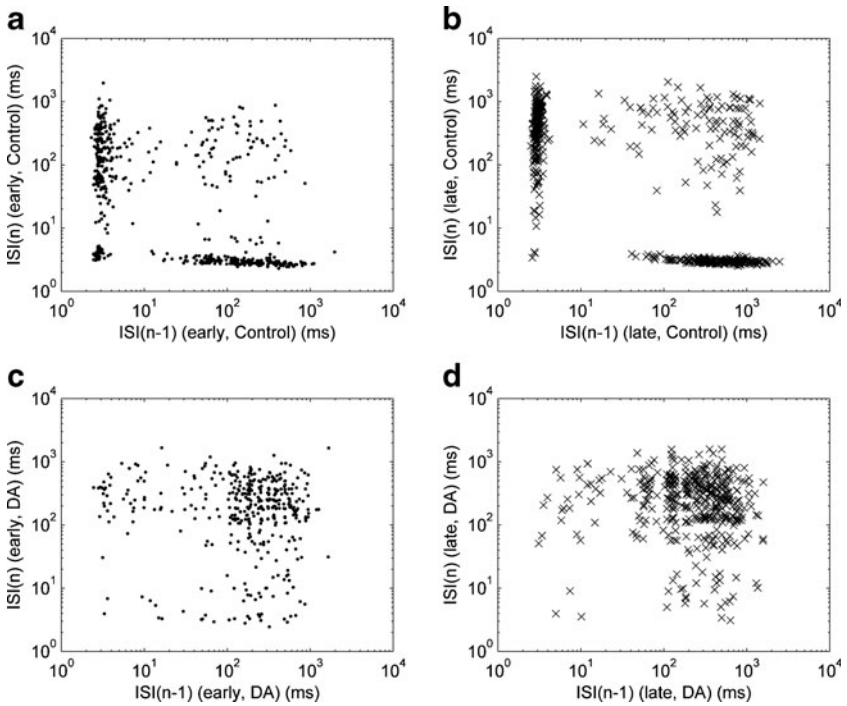

Fig. 8 Comparison of ISI distribution of one neuron firing activities in early- and late-adaptation period. (**a**) & (**b**) Previous *vs*. subsequent ISI in early-(point) and late-adaptation (cross) during control. (**c**) & (**d**) Previous *vs*. subsequent ISI in early-(point) and late-adaptation (cross) during DA application

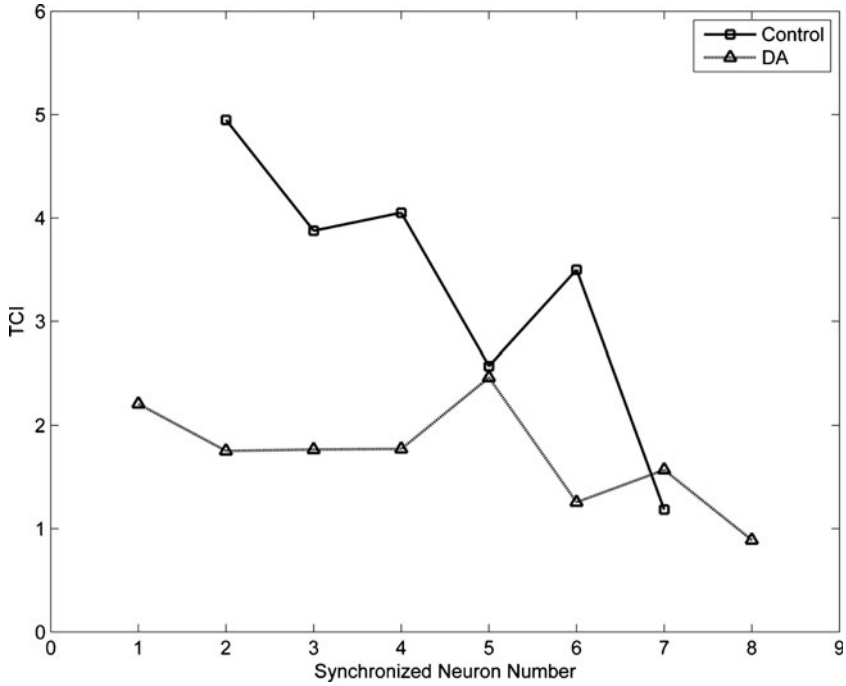

Fig. 9 Relationship between TCI and synchronized neuron number during control (*square*, *solid-line*) and DA application (*triangle*, *dash-line*)

and the burst fraction (Fig. 4b–c) and TCI values (Fig. 5) reduced. The relationship between TCI and synchronized neuron number may suggest that the effects of DA on both spatial and temporal correlation were obtained by the modulation of gap junctions among RGCs.

4.4 Mechanism of dopamine-induced changes

DA, a light-activated neuromodulator released by interplexiform cells and amacrine cells in the inner retina (Witkovsky and Dearry 1991), activates a number of intracellular pathways including cAMP-dependent protein kinase. This leads to some modification of the gap junction connexins and alters the permeability to ionic currents of gap junction (Bloomfield and Volgyi 2009).

The results found in our experiments suggested that exogenous DA-application increased the conductance of gap junction between dimming detectors, and changed the firing activities of neurons.

D1 and D2 receptors play opposite roles in intracellular phosphorylation and gap junction permeability (Bloomfield and Volgyi 2009). In our experiments, application of D2 receptor antagonist (SU) led to an increase in synchronization and a decrease in temporal correlation, which resembled the result observed in DA application. Application of D1 receptor antagonist (SCH) didn't show the same effects. Activation of D2 receptor exerted counteractive effect on activation of D1 receptor and D2 receptor would probably be desensitized by increased DA concentration (Hu et al. 2010; Callier et al. 2003). The DA-induced synchronization enhancement could be attributed to both D1 receptor activation and D2 receptor inhibition (Li et al. 2012).

Coupling of the other types of retinal neurons can also be affected by DA analogs as well. However, the neurons analyzed in this paper all had at least one synchronized neuron which was characterized by a sharp peak near zero-lag in the CCF. Two subtypes of the synchronization, dual-peak that was induced by mutual excitation between the two RGCs, and one-peak that was induced by the asymmetry or the different membrane state of two RGCs, were both mediated through gap junctions. This ensures that the effects of DA in our experiments were due to the coupling between dimming detectors to some extent.

In addition to DA-dependent gap junction modulation, DA also has multiple trophic roles in retinal function related to circadian rhythmicity, cell survival, eye growth, and so on (Witkovsky 2004). Although we cannot exclude the potential effects of other DA-related pathway that is effective in the modulation of firing activities, the effect on interneuronal gap junction is one of the most efficient ways for DA to regulate the firing activity of RGCs.

5 Conclusion

To investigate the effects of DA on firing property among neuron population, we simultaneously recorded firings of multiple dimming detectors of bullfrog retinas using multi-channel recording system. It was found that during the application of DA and SU (D2 receptor antagonist), the synchronized activities between RGCs were enhanced leading to an increase in spatial correlation, while the ISI distribution of single neuron spike trains changed remarkably and the temporal correlation in

the spike trains was reduced. On the contrary, during application of SCH (D1 receptor antagonist), the firing properties of both neuron population and single neurons showed no obvious changes. These results showed that the enhancement of gap junction conductance might be due to the activation of D1 receptor. Our results suggested that dopaminergic pathway participated in the modulation of spatial and temporal correlation of RGCs' firing activities, and may exert critical effects on visual information processing in the retina.

Acknowledgments This work was supported by the grants from the State Key Basic Research and Development Plan (No.2005CB724301) and National Foundations of Natural Science of China (No.61075108, No.60775034).

Conflicts of interest No conflict of interest

References

Baccus, S. A., & Meister, M. (2002). Fast and slow contrast adaptation in retinal circuitry. *Neuron, 36*(5), 909–919.

Bloomfield, S. A., & Volgyi, B. (2009). The diverse functional roles and regulation of neuronal gap junctions in the retina. *Nature Reviews Neuroscience, 10*(7), 495–506.

Brivanlou, I. H., Warland, D. K., & Meister, M. (1998). Mechanisms of concerted firing among retinal ganglion cells. *Neuron, 20*(3), 527–539.

Buonomano, D. V., & Maass, W. (2009). State-dependent computations: Spatiotemporal processing in cortical networks. *Nature Reviews Neuroscience, 10*(2), 113–125.

Callier, S., Snapyan, M., Le Crom, S., Prou, D., Vincent, J. D., & Vernier, P. (2003). Evolution and cell biology of dopamine receptors in vertebrates. *Biology of the Cell, 95*(7), 489–502.

Chander, D., & Chichilnisky, E. J. (2001). Adaptation to temporal contrast in primate and salamander retina. *Journal of Neuroscience, 21*(24), 9904–9916.

Chen, A. H., Zhou, Y., Gong, H. Q., & Liang, P. J. (2004). Firing rates and dynamic correlated activities of ganglion cells both contribute to retinal information processing. *Brain Research, 1017*(1–2), 13–20. doi:10.1016/j.brainres.2004.04.081.

DeVries, S. H. (1999). Correlated firing in rabbit retinal ganglion cells. *Journal of Neurophysiology, 81*(2), 908–920.

Field, G. D., & Chichilnisky, E. J. (2007). Information processing in the primate retina: Circuitry and coding. *Annual Review of Neuroscience, 30*, 1–30. doi:10.1146/annurev.neuro.30.051606.094252.

Hampson, E. C., Vaney, D. I., & Weiler, R. (1992). Dopaminergic modulation of gap junction permeability between amacrine cells in mammalian retina. *Journal of Neuroscience, 12*(12), 4911–4922.

Hosoya, T., Baccus, S. A., & Meister, M. (2005). Dynamic predictive coding by the retina. *Nature, 436*(7047), 71–77.

Hu, E. H., Pan, F., Volgyi, B., & Bloomfield, S. A. (2010). Light increases the gap junctional coupling of retinal ganglion cells. *The Journal of Physiology, 588*(Pt 21), 4145–4163.

Jing, W., Liu, W. Z., Gong, X. W., Gong, H. Q., & Liang, P. J. (2010). Visual pattern recognition based on spatio-temporal patterns of retinal ganglion cells' activities. *Cogn Neurodyn, 4*(3), 179–188. doi:10.1007/s11571-010-9119-8.

Koch, K., McLean, J., Berry, M., Sterling, P., Balasubramanian, V., & Freed, M. A. (2004). Efficiency of information transmission by retinal ganglion cells. *Current Biology, 14*(17), 1523–1530. doi:10.1016/j.cub.2004.08.060.

Krahe, R., & Gabbiani, F. (2004). Burst firing in sensory systems. *Nature Reviews Neuroscience, 5*(1), 13–23. doi:10.1038/nrn1296.

Lesica, N. A., & Stanley, G. B. (2004). Encoding of natural scene movies by tonic and burst spikes in the lateral geniculate nucleus. *Journal of Neuroscience, 24*(47), 10731–10740.

Lettvin, J. Y., Maturana, H. R., McCulloch, W. S., & Pitis, W. H. (1959). What the frog's eye tells the Frog's brain. *Proceedings of the IRE, 47*, 1940–1951.

Li, H., Liu, W. Z., & Liang, P. J. (2012). Adaptation-dependent synchronous activity contributes to receptive field size change of bullfrog retinal ganglion cell. *PLoS One, 7*(3), e34336. doi:10.1371/journal.pone.0034336.

Lisman, J. E. (1997). Bursts as a unit of neural information: Making unreliable synapses reliable. *Trends in Neurosciences, 20*(1), 38–43.

Liu, W. Z., Jing, W., Li, H., Gong, H. Q., & Liang, P. J. (2011a). Spatial and temporal correlations of spike trains in frog retinal ganglion cells. *Journal of Computational Neuroscience, 30*(3), 543–553. doi:10.1007/s10827-010-0277-9.

Liu, W. Z., Yan, R. J., Jing, W., Gong, H. Q., & Liang, P. J. (2011b). Spikes with short inter-spike intervals in frog retinal ganglion cells are more correlated with their adjacent neurons' activites. *Protein & Cell, 2*, 764–771.

Liu, X., Zhou, Y., Gong, H. Q., & Liang, P. J. (2007). Contribution of the GABAergic pathway(s) to the correlated activities of chicken retinal ganglion cells. *Brain Research, 1177*, 37–46.

Meister, M., Lagnado, L., & Baylor, D. A. (1995). Concerted signaling by retinal ganglion cells. *Science, 270*(5239), 1207–1210.

Metzner, W., Koch, C., Wessel, R., & Gabbiani, F. (1998). Feature extraction by burst-like spike patterns in multiple sensory maps. *Journal of Neuroscience, 18*(6), 2283–2300.

Mills, S. L., Xia, X. B., Hoshi, H., Firth, S. I., Rice, M. E., Frishman, L. J., et al. (2007). Dopaminergic modulation of tracer coupling in a ganglion-amacrine cell network. *Visual Neuroscience, 24*(4), 593–608.

Pillow, J. W., Shlens, J., Paninski, L., Sher, A., Litke, A. M., Chichilnisky, E. J., et al. (2008). Spatio-temporal correlations and visual signalling in a complete neuronal population. *Nature, 454*(7207), 995–999.

Reid, R. C., Victor, J. D., & Shapley, R. M. (1997). The use of m-sequences in the analysis of visual neurons: Linear receptive field properties. *Visual Neuroscience, 14*(6), 1015–1027.

Reinagel, P., Godwin, D., Sherman, S. M., & Koch, C. (1999). Encoding of visual information by LGN bursts. *Journal of Neurophysiology, 81*(5), 2558–2569.

Reinagel, P., & Reid, R. C. (2000). Temporal coding of visual information in the thalamus. *Journal of Neuroscience, 20*(14), 5392–5400.

Ribelayga, C., Cao, Y., & Mangel, S. C. (2008). The circadian clock in the retina controls rod-cone coupling. *Neuron, 59*(5), 790–801.

Schnitzer, M. J., & Meister, M. (2003). Multineuronal firing patterns in the signal from eye to brain. *Neuron, 37*(3), 499–511.

Strong, S. P., de Ruyter van Steveninck, R. R., Bialek, W., & Koberle, R. (1998). On the application of information theory to neural spike trains. *Pac Symp Biocomput*, 621–632.

Swadlow, H. A., & Gusev, A. G. (2001). The impact of 'bursting' thalamic impulses at a neocortical synapse. *Nature Neuroscience, 4*(4), 402–408. doi:10.1038/86054.

Teich, M. C., Turcott, R. G., & Siegel, R. M. (1996). Temporal correlation in cat striate-cortex neural spike trains. *Engineering in Medicine and Biology Magazine, IEEE, 15*(5), 79–87.

Usrey, W. M., Reppas, J. B., & Reid, R. C. (1999). Specificity and strength of retinogeniculate connections. *Journal of Neurophysiology, 82*(6), 3527–3540.

Wang, G. L., Zhou, Y., Chen, A. H., Zhang, P. M., & Liang, P. J. (2006). A robust method for spike sorting with automatic overlap decomposition. *IEEE Transactions on Biomedical Engineering, 53*(6), 1195–1198. doi:10.1109/TBME.2006.873397.

Witkovsky, P. (2004). Dopamine and retinal function. *Documenta Ophthalmologica, 108*(1), 17–40.

Witkovsky, P., & Dearry, A. (1991). Functional roles of dopamine in the vertebrate retina. *Progress in Retinal Research, 11*, 247–292.

Witkovsky, P., Nicholson, C., Rice, M. E., Bohmaker, K., & Meller, E. (1993). Extracellular dopamine concentration in the retina of the clawed frog, xenopus laevis. *Proceedings of the National Academy of Sciences of the United States of America, 90*(12), 5667–5671.

Zhang, P. M., Wu, J. Y., Zhou, Y., Liang, P. J., & Yuan, J. Q. (2004). Spike sorting based on automatic template reconstruction with a partial solution to the overlapping problem. *Journal of Neuroscience Methods, 135*(1–2), 55–65. doi:10.1016/j.jneumeth.2003.12.001.